Transmission electron microscopy observation of the half-Heusler compound $Ti_{0.5}(Zr_{0.5}Hf_{0.5})_{0.5}NiSn_{0.998}Sb_{0.002}$

Takao Morimura[a,*], Masayuki Hasaka[b] and Shin-ichiro Kondo[b]

[a]Graduate School of Science and Technology, Nagasaki University, 1-14 Bunkyo-machi, Nagasaki 852-8521, Japan

[b]Department of Materials Science and Engineering, Faculty of Engineering, Nagasaki University, 1-14 Bunkyo-machi, Nagasaki 852-8521, Japan

*Corresponding author. Tel.: +81-95-819-2636; Fax: +81-95-819-2634

E-mail address: tmori@nagasaki-u.ac.jp (T. Morimura)

Abstract

High-performance thermoelectric compound $Ti_{0.5}(Zr_{0.5}Hf_{0.5})_{0.5}NiSn_{0.998}Sb_{0.002}$ with half-Heusler lattice was measured and observed by an XRD and a TEM. Each half-Heusler peak in the XRD pattern accompanied a bump at the high-angle side. Granular domains, a few nanometer in dimension, were observed in a bright-field TEM image. A Fourier-transformation and an inverse Fourier-transformation for the HRTEM image revealed that the granular structure consists of the half-Heusler domains with ordering and with disordering between second nearest neighbor atoms.

Keywords: High resolution electron microscopy; half-Heusler phase; melt spinning; X-ray diffraction; Thermoelectric material

Half-Heusler compound TiNiSn is a prospective material for thermoelectric conversion, which has an $F\bar{4}3m$ symmetry and a lattice constant 0.594 nm. The unit cell consists of four interpenetrating FCC sublattices of α-site, β-site, γ-site and δ-site, which are occupied by Ti, Ni, Sn and vacancy, respectively (Fig.1). The thermoelectric properties are strongly dependent on the microstructure and the atomic configuration. The atomic substitution by additional element, the atomic disordering and the partial occupation of a vacancy-site are easily allowed in this structure. High performances for the thermoelectric conversion were previously presented in $Zr_{0.5}Hf_{0.5}NiSn_{0.99}Sb_{0.01}$ [1], $Zr_{0.5}Hf_{0.5}Ni_{0.8}Pd_{0.2}Sn_{0.99}Sb_{0.01}$ [2,3] and $Ti_{0.5}(Zr_{0.5}Hf_{0.5})_{0.5}NiSn_{0.998}Sb_{0.002}$ [4] by the atomic substitutions. And the partial vacancy-occupation of the Co, Sn and Ni atoms was reported in Ti-Co-Sn [5-7] and the Ti-Ni-Sn [8] systems. In the present work, the high performance thermoelectric compound $Ti_{0.5}(Zr_{0.5}Hf_{0.5})_{0.5}NiSn_{0.998}Sb_{0.002}$, reported in [4], was observed and measured by an X-ray diffraction (XRD) and a transmission electron microscope (TEM).

Mixtures of pure metals were melted in a high-frequency induction furnace in an argon atmosphere to produce an alloy with the composition of $Ti_{0.5}(Zr_{0.5}Hf_{0.5})_{0.5}NiSn_{0.998}Sb_{0.002}$. The ingot was melted and rapidly cooled by spin-cast on copper roll with circumferential velocity of 10m/s. The spin-cast ribbon was annealed at 1000 K for 172.8 ks and subsequently quenched to iced brine. For the XRD sample, the ribbon was ground into powders (~75 μm). The phases were identified from XRD patterns by using a Rigaku RINT-2200V. For the TEM sample, the ribbon was mounted on a copper single hole grid with 3 mm diameter and then thinned by Ar^+ beam accelerated at 5 kV in an incident angle of 10^o. TEM observations were performed at an accelerating voltage of 200 kV using a JEOL JEM-2010 at Joint Research Center in Nagasaki University. A Fourier-transformation and an inverse Fourier-transformation were performed for high-resolution (HR) TEM images.

Fig.2 shows X-ray diffraction pattern of $Ti_{0.5}(Zr_{0.5}Hf_{0.5})_{0.5}NiSn_{0.998}Sb_{0.002}$ spin-cast and subsequently annealed at 1000K for 172.8ks. Most diffraction peaks are indexed as the half-Heusler structure, although weak peaks different from the half-Heusler are observed as shown by full circles. Each

half-Heusler peak is asymmetry and accompanies a bump at the high-angle side. The same result was obtained in [9], where the structure is reported as the mixture of Ti-rich and Ti-poor half-Heusler grains, several micrometer in dimension. The same kind of structure seems to occur also in the present sample despite the spin-cast fabrication.

Fig.3 shows a bright field TEM image and the diffraction pattern. A large crystal grain, several micrometer in dimension, was observed, which are not shown in Fig.3. Granular contrasts, a few nanometer in dimension, are observed within the crystal grain. The bumps in Fig.2 are not attributed to the granular domains because the Ti-rich and the Ti-poor grains are much larger in [9]. The diffraction pattern was indexed as [110] electron incidence for the half-Heusler structure.

Fig.4 (a) shows a HRTEM image at the [110] electron incidence at a Scherzer focus of an object lens. A lot of spots, corresponding to atomic alignments of the half-Heusler lattice, are observed. Bright and dark contrasts, a few nanometer in dimension, corresponding to the granular contrasts in Fig.3, are observed. The atomic alignments in the bright and the dark domains seem to be coherent in Fig.4 (a). Fig.4 (b) shows a Fourier-transformed image from a square in (a). The image (b) confirms that whole square area in (a) consists of the half-Heusler phase oriented along [110] direction.

In order to observe the (002), (220) and (111) atomic planes, the inverse Fourier-transformed images were shown in Fig.5. The inverse Fourier-transformation was performed by using 002 and $00\bar{2}$ spots (a), by using 220 and $\bar{2}\,\bar{2}\,0$ spots (b) and by using $11\bar{1}$ and $\bar{1}\,\bar{1}\,1$ spots (c). The (002) and the (220) fringes are clearly observed over the whole area of (a) and (b), respectively, although slightly weakened fringes are partially observed in (a). On the other hand, the fringe-free domains, a few nanometer in dimension, are observed in Fig.5 (c), which are as large as the granular contrasts observed in Fig.3.

The structure factors for 220, 002 and 111 reflections are estimated as

$$F_{220} = 4(f_\alpha + f_\beta + f_\gamma + f_\delta),$$

$$F_{002} = 4\{(f_\alpha + f_\gamma) - (f_\beta + f_\delta)\},$$

$$F_{111} = 4\{(f_\alpha - f_\gamma)^2 + (f_\beta - f_\delta)^2\}^{1/2},$$

where f_α, f_β, f_γ and f_δ indicate the atomic scattering factors averaged on α-, β-, γ- and δ-sites of Fig.1, respectively [10]. The 002 reflection is attributed to the ordering between the first nearest neighbor (α, γ)-site and (β, δ)-site. The 111 reflection is attributed to the ordering between the second nearest neighbor α-site and γ-site, or between β-site and δ-site. The 220 reflection is fundamental and F_{220} isn't dependent on the atomic configurations. Fig.5 (a) and (b) indicate that the fundamental lattice and the ordering between the first nearest neighbor atoms are almost retained over the square area of Fig.3 (a), although slight disordering or slight composition variation may occur as in Fig.5 (a). On the other hand, the fringe-free domains in Fig.5(c) are clearly attributed to the disordering between the second nearest neighbor atoms.

Two causes for the fringe-free domains in Fig.5(c) can be considered from the expression of F_{111}. One is the disordering between the second nearest neighbour Ni atoms and vacancies, and another is the disordering between the Ti atoms and the Sn atoms. In order to examine the causes, the F_{111} was estimated with changing the distribution ratio of Ni to the vacancy, p_v. The results for the $Ti_{0.5}(Zr_{0.5}Hf_{0.5})_{0.5}NiSn$ are shown in Fig.6 by using the atomic scattering factors presented by Smith et al. [11]. The p_v=0.5 means the perfect disordering between the Ni atoms and the vacancies. The F_{111} has minimum at p_v=0.5 and are very small. The residual value of F_{111} at p_v=0.5 is attributed to the perfect ordering between the second nearest neighbour Ti atoms and Sn atoms, which slightly contribute to the 111 reflection. Therefore the disordering between the Ni atoms and the vacancies is more effective for weakening the 111 reflection than the disordering between the Ti atoms and the Sn atoms. It is possible

that the granular structure in Fig.3 consists of two kinds of domains, one is the ordered half-Heusler and another is the half-Heusler in which Ni partially occupies the vacancy.

In summary, we demonstrated the microstructure of thermoelectric compound $Ti(Zr_{0.5}Hf_{0.5})_{0.5}NiSn_{0.998}Sb_{0.002}$ with the half-Heusler lattice by an XRD and a TEM. The XRD pattern was indexed as the half-Heusler structure in the sample spin-cast and subsequently annealed at 1000K for 172.8ks. Each half-Heusler peak accompanies a bump in the high-angle side. Granular domains, a few nanometer in dimension, were observed in a bright field TEM image. From a Fourier-transformation and an inverse Fourier-transformation for the HRTEM image revealed that the granular structure consists of the half-Heusler domains with ordering and with disordering between second nearest neighbor atoms.

References

[1] C. Uher, J. Yang, S. Hu, D.T. Morelli, G.P. Meisner, Phys. Rev. B 59 (1999) 8615.

[2] Q. Shen, L. Chen, T. Goto, T. Hirai, J. Yang, G. P. Meisner, C. Uher, Appl. Phys. Lett. 79 (2001) 4165.

[3] Q. Shen, L. Zhang, L. Chen, T. Goto, T. Hirai, J. Mater. Sci. Lett. 20 (2001) 2197.

[4] N. Shutoh, S. Sakurai, J. Alloys Compd 389 (2005) 204.

[5] R. V. Skolozdra, Yu V. Stadnyk, Yu K. Gorelenko, E. É. Teletskaya, Sov. Phys. Solid State 32 (1990) 1536.

[6] T. Nobata, G. Nakamoto, M. Kurisu, Y. Makihara, T. Tokuyoshi, I. Nakai, Jpn. J. Appl. Phys. 38 (1999) 429.

[7] T. Nobata, G. Nakamoto, M. Kurisu, Y. Makihara, K. Ohoyama, M. Ohashi, J. Alloy Compd. 347 (2002) 86.

[8] T. Morimura, M. Hasaka, Ultramicroscopy 106 (2006) 553.

[9] K. Kurosaki, T. Maekawa, H. Muta, S. Yamanaka, J. Alloy Compd. 397 (2005) 296.

[10] G. Andre, F. Bouree, A. Oles, A. Szytula, Solid State Commun. 93 (1995) 139.

[11] G.H. Smith, R.E. Burge, Acta Cryst. 15 (1962) 182.

Figure captions

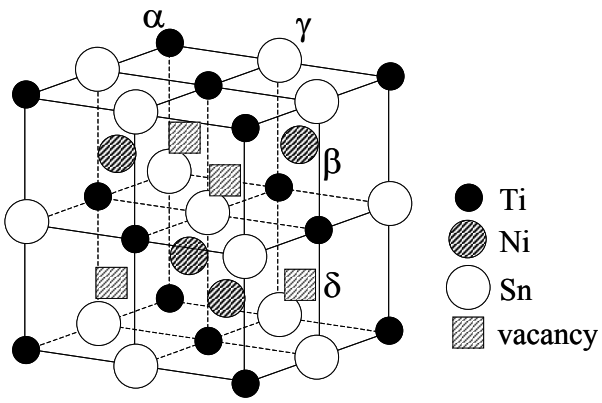

Fig.1 Unit cell of half-Heusler TiNiSn.

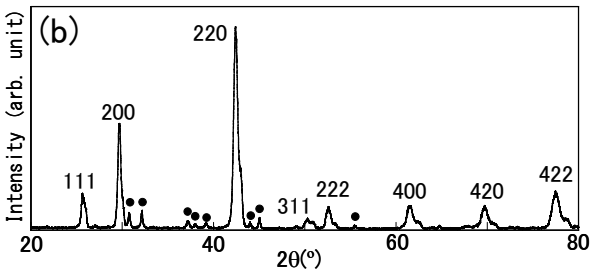

Fig.2 X-ray diffraction patterns of $Ti_{0.5}(Zr_{0.5}Hf_{0.5})_{0.5}NiSn_{0.998}Sb_{0.002}$ spin-cast and subsequently annealed at 1000K for 172.8 ks. The diffraction peaks are indexed as a half-Heusler lattice except the weak peaks shown by full circles.

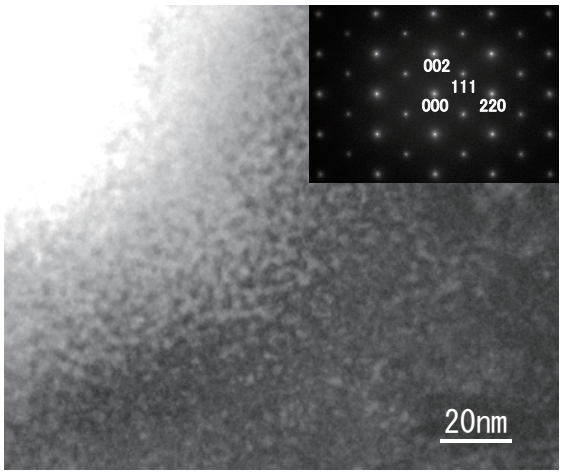

Fig.3 Bright field TEM image of $Ti_{0.5}(Zr_{0.5}Hf_{0.5})_{0.5}NiSn_{0.998}Sb_{0.002}$ spin-cast and subsequently annealed at 1000K for 172.8 ks. The diffraction pattern at a [110] electron incidence is inset.

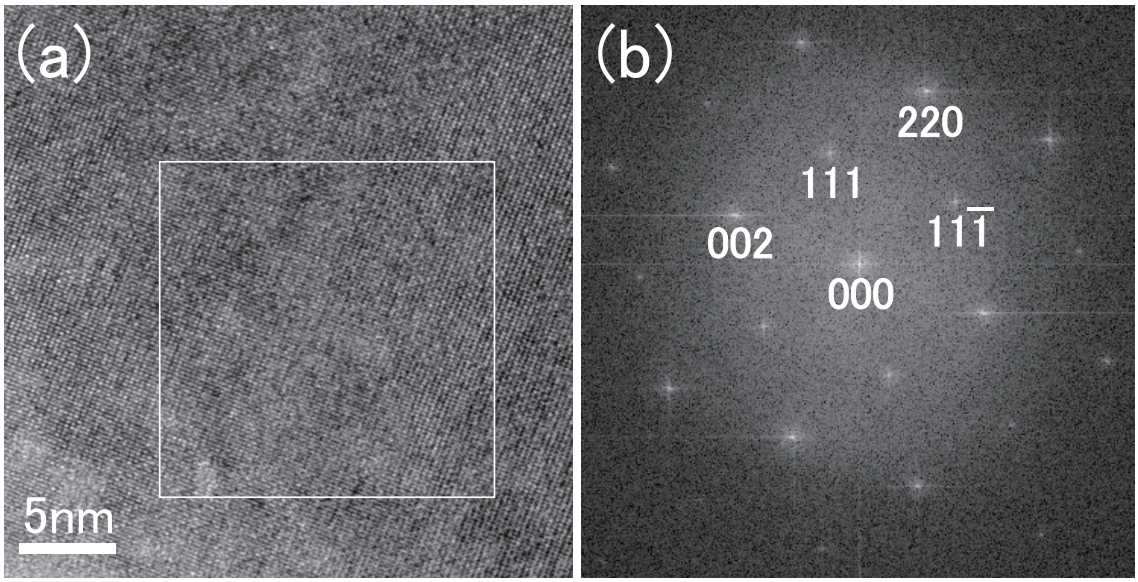

Fig.4 High-resolution TEM image of a $Ti_{0.5}(Zr_{0.5}Hf_{0.5})_{0.5}NiSn_{0.998}Sb_{0.002}$ spin-cast and subsequently annealed at 1000K for 172.8 ks (a) and Fourier-transformed image for the square area (b).

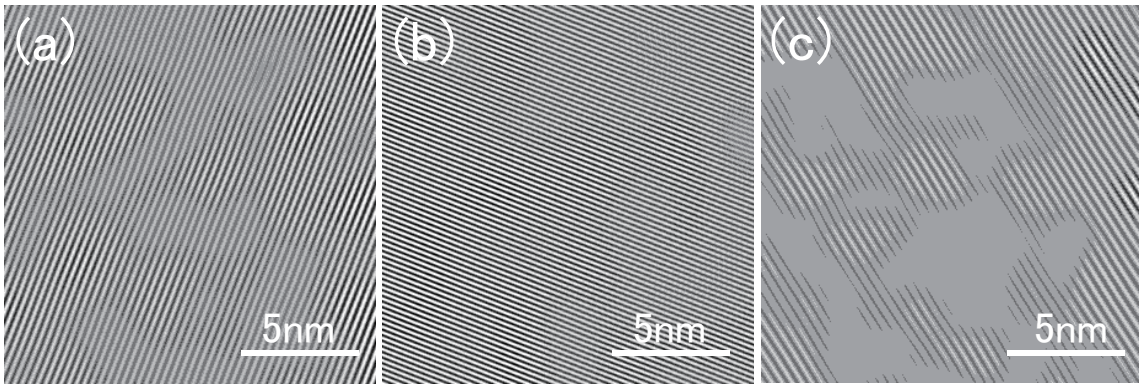

Fig.5 Inverse Fourier-transformed images obtained by 002 and $00\bar{2}$ spots (a), by 220 and $\bar{2}\,\bar{2}\,0$ spots (b) and by $11\bar{1}$ and $\bar{1}\,\bar{1}\,1$ spots (c) in Fig.3 (b).

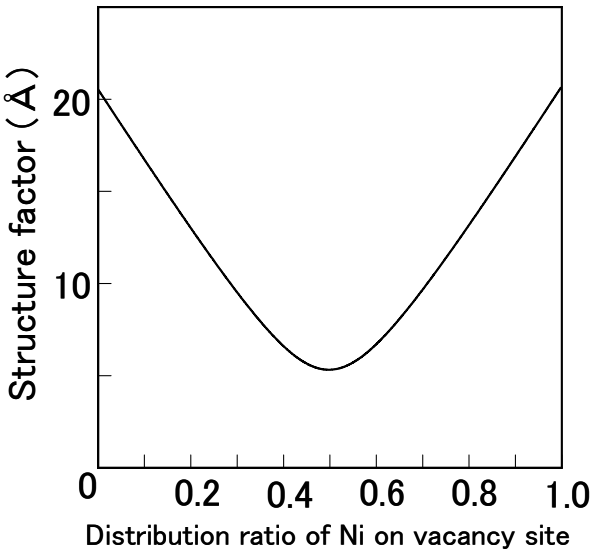

Fig.6 Structure factor of 111 reflection estimated with the distribution ratio of Ni on vacancy-site in $Ti_{0.5}(Zr_{0.5}Hf_{0.5})_{0.5}NiSn$.